Faraday Discussions

Accepted Manuscript

This manuscript will be presented and discussed at a forthcoming Faraday Discussion meeting. All delegates can contribute to the discussion which will be included in the final volume.

Register now to attend! Full details of all upcoming meetings: http://rsc.li/fd-upcoming-meetings

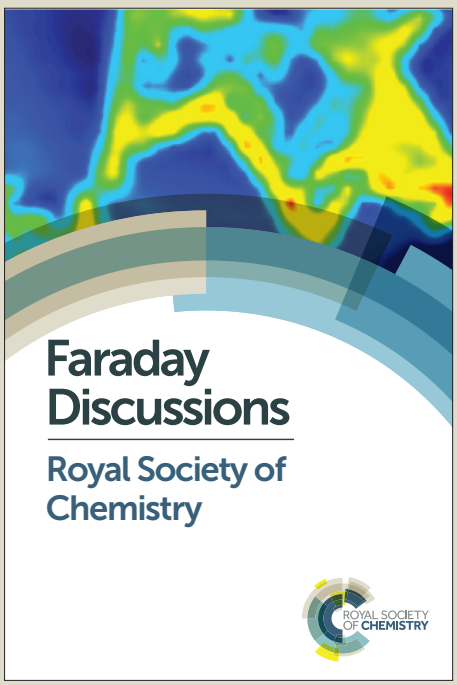

This is an *Accepted Manuscript*, which has been through the Royal Society of Chemistry peer review process and has been accepted for publication.

Accepted Manuscripts are published online shortly after acceptance, before technical editing, formatting and proof reading. Using this free service, authors can make their results available to the community, in citable form, before we publish the edited article. We will replace this *Accepted Manuscript* with the edited and formatted *Advance Article* as soon as it is available.

You can find more information about *Accepted Manuscripts* in the Information for Authors.

Please note that technical editing may introduce minor changes to the text and/or graphics, which may alter content. The journal's standard Terms & Conditions and the Ethical guidelines still apply. In no event shall the Royal Society of Chemistry be held responsible for any errors or omissions in this *Accepted Manuscript* or any consequences arising from the use of any information it contains.

ROYAL SOCIETY OF CHEMISTRY

www.rsc.org/faraday_d

Kinetics of Aggregation and Growth Processes of PEG-Stabilised Mono- and Multivalent Gold Nanoparticles in Highly Concentrated Halide Solutions

Benjamin Stein,[a] David Zopes,[b] Madlen Schmudde,[a] Ralf Schneider,[a] Ahmed Mohsen,[a] , Christian Goroncy,[a] Sanjay Mathur,[b] and Christina Graf[a]*

DOI: 10.1039/b000000x

5-6 nm gold nanoparticles were prepared by hydrolytic decomposition of $[NMe_4][Au(CF_3)_2]$ and in situ functionalized with mono- and multivalent thiolated PEG ligands. Time-dependent changes of the nanoparticles were monitored in aqueous NaCl, NaBr, and NaI solutions by UV-Vis spectroscopy, TEM, and HRTEM. The purely sterically protected particles are stable in ≤1 M NaCl and NaBr solutions regardless of the valence of the ligands. At higher concentrations (≥ 2 M), the monovalent stabilized particles show minor reaction limited colloidal aggregation. In NaBr but not in NaCl solutions additionally a minor Ostwald ripening occurs. The divalent stabilized particles remain colloidally stable in both halide solutions even if the temperature is raised or the concentration is increased above 2 M. In ≤1 M aqueous NaI solutions the particles remain stable. Above, the monovalent stabilized particles undergo an oxidative reaction resulting in a time-dependent shift and broadening of the absorbance spectrum. Finally, this process slows down while the width of the spectra slightly narrows. The kinetics of this process can be described by a two-step sigmoidal process comprising a slow induction period where active species are formed, followed by a fast growth and aggregation process. The increasing concentration of fused structures from the aggregates during this process results in a narrowing of the size distributions. The divalent stabilized particles show only some minor broadening and a slight shift of the absorbance spectra in ≤ 3 M NaI solutions. These observations confirm the excellent stability of the multivalent stabilized particles from this chloride-free particle synthesis.

[a] Institut für Chemie u. Biochemie, Freie Universität Berlin, Takustraße 3, 14195 Berlin, Germany
[b] Department für Chemie, Lehrstuhl für Anorganische und Materialchemie, Universität zu Köln, Greinstraße 6, 50939 Köln, Germany

Introduction

The stability of metal nanoparticles in salt solutions is a key criterion for their usage in many applications, especially in life science. Interaction of halides with electrostatically stabilized gold nanoparticles leads at low ion concentrations to severe aggregation due to the reduction of the electrostatic bilayer. Such particles aggregate already at NaCl concentrations of 100 mM, which is less than the NaCl concentration in standard cell culture media.[1] The stability of electrostatically as well as sterically stabilized metal nanoparticles can be further reduced by the exchange of the ligands by halides. The affinity of the halides to gold increases from fluoride to iodide according to the HSAB concept, since gold is a soft acid, and iodide among the halides, the softest and fluoride the hardest base.[2] Accordingly, the stability of Au (I) and Au (III) halogenide complexes increases from chloride to iodide about 10 and 20 orders of magnitude, respectively.[3] The binding energy of halogenides to gold increases with increasing polarizability of the ions (I^-> Br^-> Cl^-), as well.[4, 5] Consequently, the presence of halide ions in dispersions of gold nanoparticles may lead to aggregation and possible growth processes that are dependent on the used halides. Liu et al. observed that the addition of a 0.1 M solution of NaF or NaCl to electrostatically stabilized, glutamic acid-protected gold nanoparticles results in a different effect than the addition of NaBr and NaI.[6] Fluoride and chloride are too weak to replace the glutamic acid on the gold surface so that their addition only causes a reduction of the protective electrostatic double layer on the gold nanoparticles which leads to aggregation of the nanoparticles. Bromide and iodide have a stronger affinity to gold and therefore replace more glutamic acid from the gold nanoparticle surface and consequently the aggregation process is faster, the fastest process is found for NaI. Finally, pearl-chain-like 3 D nanostructures are found. In the presence of iodide and bromide, the diameters of the individual gold nanoparticles in the aggregates are partially bigger and partially smaller than in the original dispersion, whereas the presence of NaCl does not affect the particle size.[6] Similar specific effects of the halides were observed by Singh et al. [7], although these authors investigated octadecylamine-protected gold nanoparticles in organic media, such as chloroform or toluene. Significant changes were already found in 10^{-4} M solutions of the halogenide succinimides. Here, too, the presence of bromide and iodide significantly changed the diameters of the individual gold nanoparticles where larger and smaller particles including rather irregular structures were found. Whether the latter structures resulted from fusion or aggregation and growth processes was not revealed. In contrast, in the presence of chloride merely an aggregation of the particles took place. Dramatic changes of the extinction spectra were only found for iodide, where a red shift of the maximum and a broadening of the plasmon band are clearly visible. The spectra of the gold nanoparticles in the presence of the other halides are only slightly different from those of the starting material. This difference arises from the fact that the particles formed during the reaction with iodide are much larger than those formed in the reaction with bromide. The observed effects are explained by lattice strain effects as a result of halide ion adsorption on the Au(111) planes and in the case of iodine by the formation of AuI on the surfaces. Neither for ref. [6] nor for ref. [7] a systematic study on the kinetics of the aggregation and growth processes was reported. The mechanism of the reaction between KI and 12 nm, citrate-stabilized gold nanoparticles proceeds according to Cheng et al. by a chemisorptive process.[8] An energetic injection of the chemisorbed iodide ($I^- - e^- \rightarrow I(adsorbed) + e^-$)

on the gold nanoparticle surface enables an exchange of gold monomers between the individual nanoparticles.[8] The authors concluded from the observed spectra and TEM images that a fusion of the particles takes place. [8] Dasog et al. showed that gold nanoparticles (from a Brust-Schiffrin synthesis) can be oxidized and dissolved in the presence of tetraoctyl ammonium bromide and oxygen. Here, a sequential oxidation of the gold-bound thiol groups to disulfide and sulfonate together with an oxidation of Au^0 atoms to Au^{3+} species takes place.[9] These reactions are accompanied by an Ostwald ripening. Already at bromide concentrations above 0.20 M the gold nanoparticles are completely oxidized and dissolve.[9] Liu et al. studied by HRTEM the junctions between individual particles in aggregate-like structures that were formed by the reaction between glutamic acid-stabilized gold colloids and bromide or iodide, respectively. From this observation, they concluded that a fusion and not simply an aggregation takes place.[6] The spacing in the grating plane in the connecting regions of these aggregates is 0.230 nm, which corresponds to a (111) crystal plane and demonstrates the crystallinity of this joint.[6] Also Pei et al. described a fusion mechanism and confirmed it with HRTEM measurements, in studying the formation of nanowires in a citrate-based reduction reaction with chloroauric acid as gold precursor. [10, 11] Pei et al. propose a mechanism where first van der Waals attractions between two gold nanoparticles leads to adhesion. The fusion is then caused by the selective deposition of gold compounds on the concave surface between two attached gold nanoparticles.[11] It is known that halides, can strongly influence the 1-D growth of metal nanoparticles.[12, 13] The iodide concentration plays a pivotal role in the resulting morphology in the formation of anisotropic gold particles using the cetyltrimethylammonium bromide (CTAB) synthesis route.[13] Ha et al. synthesized trigonal gold nanoprisms by the addition of iodide in the CTAB synthesis.[14] Halide ions adsorb on gold surfaces with binding energies which depend on the polarizability (I-> Br-> Cl-) and the crystal lattice planes ((111)> (110)> (100)).[4] Ha et al. suggest, that iodide binds specifically to the (111) lattice plane of gold, so that the crystal growth on the (100) - and (110) lattice planes is promoted. Also a modified Turkevich approach[15] with halide additives leads to triangular nanostructures.[16] It was shown in this synthesis that chloride leads to the formation of nanoprisms, while bromide and iodide inhibit the growth of nanoprisms. In most studies where halides are applied for shape control their concentration is low (10-100 μM. At higher concentrations, the effects discussed above dominate.

The aggregation kinetics of electrostatic stabilized metal nanoparticles in the presence of electrolytes have been widely investigated, including various studies for gold and silver particles in the presence of halides, mostly for halide concentrations of 0.1 M or less.[17-20] Whereas for some systems kinetics in agreement with the classical Derjaguin–Landau–Verwey–Overbeek (DLVO) theory and processes in both the reaction-limited and diffusion-limited regimes were found,[17, 18, 20, 21] for other particle systems significant deviations from this theory are reported.[18, 19] The kinetics of the aggregation of sterically stabilized metal nanoparticles was rarely studied. At NaCl concentrations above 7 M, polyvinylpyrrolidone-stabilized silver nanoparticles show a time dependent aggregation, which is not in agreement with DLVO theory. [18] Most studies on fusion processes between noble metal nanoparticles are focused on the formation of the crystals, not the kinetics. Morita et al. investigated the time dependence of the fusion growth of gold nanoparticles induced by the conformational change of a thermoresponsive polymer by SAXS and TEM.[22] Thereby, it turned out, that the particle size reaches its maximum not

in the final stage but in the middle stage, which the authors explained by a shrinkage of initially formed aggregates due to fusion processes.[22]

We have recently shown that in situ functionalization of gold nanoparticles from a Cl^--free synthesis with mono- and multivalent thiol polyethylene glycol (PEG) ligands leads to purely sterically stabilized nanoparticles with an up to two orders of magnitude enhanced stability under harsh conditions compared to gold nanoparticles from a syntheses comprising the reduction of $HAuCl_4$ and subsequent ligand exchange.[23] This high stability is due to the fact that in the absence of chloride a higher percentage of the gold atoms on the particle surface are protected by strongly binding thiol ligands than in approaches where chloride is present during particle formation. These particles are also stable in 3 M aqueous solutions of NaCl, where particles stabilized by bi- or trivalent stabilized thiol ligands are much more stable than those with monovalent ligands.[23] These nanoparticles are ideal model systems for studies on the influence of halides on the stability and shape evolution of gold nanoparticles initially independent from electrostatic effects. Here, we present a systematic study on the aggregation and growth mechanisms of these particles in aqueous solutions of NaCl, NaBr, and NaI. The kinetics of the reactions are studied by absorbance spectroscopy and complementary electron microscopy studies.

Results and Discussion

Gold nanoparticles were prepared by hydrolytic decomposition of $[NMe_4][Au(CF_3)_2]$[24] and in situ functionalized with mono-, di- and trivalent thiolated PEG ligands (see Figure S1 in the Supporting Information).[23] In this way several batches of spherical gold nanoparticles with about 5-6 nm diameter and a polydispersity of 10-20% were obtained. Due to the chloride-free synthesis and the neutral methoxy end groups of their thiol ligands, the particles have a zetapotential around zero (between -2.2±0.5 mV and -5.5±0.5 mV for different batches). A typical TEM image of these particles is shown in Figure S2 in the Supporting Information.

Studies in NaCl and NaBr

All investigated nanoparticles are stable at NaCl concentrations below 1 M for at least 24 h. In higher concentrated NaCl solutions the monovalent stabilized nanoparticles show minor aggregation leading to some minor precipitation resulting in a slight reduction of the intensity of the absorbance spectra with time (see e. g. data for a 3 M solution of NaCl in Figure 1). However, neither the maximum of the plasmon resonance band is shifted nor the spectra are broadened. TEM measurements confirm that no changes in size and morphology occur. Di- or trivalent stabilized nanoparticles are not aggregating in ≤3 M NaCl and their plasmon resonance spectra remain unchanged after 96 h of treatment with 3 M NaCl. At even higher concentration (5 M) minor aggregation occurs leading to a broadening and a red shift of the plasmon resonance spectrum (see ref. [23]). However, even under these conditions no changes in size and morphology occur after 4 months in NaCl regardless of the valence of the ligand. Thus all spectral changes observed in aqueous solution of NaCl are purely due to (minor) aggregation.

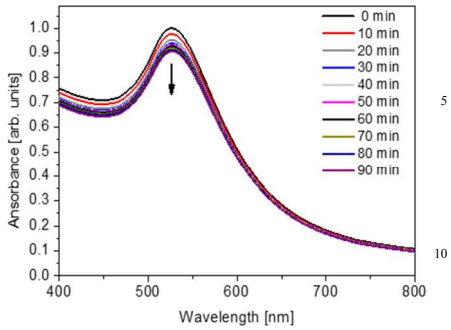

Figure 1. (a) Time-dependent changes of absorbance spectra of monothiol PEG-stabilized gold nanoparticles in a 3 M aqueous solution of NaCl at 25°C.

In order to check whether a significant release of thiol ligands occurs during the interaction with the salt solutions, the monovalent stabilized gold nanoparticles were separated from the salt solution at different times during the reaction, to stop the reaction and to determine the amount of thiols that remains on the colloids by ICP-OES (see Experimental). For each sample the Au:S ratio was calculated and compared with the value for the untreated particles. The data for 2 M sodium halide solutions at 25° C are summarized in Table 1. In case of NaCl, this data confirm that the Au: S ratio even after 48 h does not change, which indicates that only a negligible number of ligands is released due to the interaction with chloride. In addition, it was also checked whether gold is found in the remaining salt solution, however large amounts of sodium cause ionization interferences with gold, so that an exact reproducible determination of the gold concentration was impossible but these measurements indicate that even in NaCl solutions some gold is released and that the amount of gold increases from chloride to bromide to iodide.

Table 1 Au:S ratio determined by ICP-OES of monovalent stabilized nanoparticles separated from 2 M sodium halide solutions at 25°C after 2 h and 48 h compared to an untreated control sample

Halide solution	Au:S ratio	
	2 h	48 h
Control	2.9 ± 0.2	2.9 ± 0.2
NaCl	2.9 ± 0.2	2.9 ± 0.2
NaBr	3.5 ± 0.2	5.0 ± 0.2
NaI	4.5 ± 0.2	--

Bromide has a significantly higher affinity to gold than chloride,[3-5] therefore a more important influence on the colloidal stability of the gold nanoparticles for NaBr than for NaCl is expected. From the chemistry of gold extraction it is known that gold can be dissolved in aqueous bromine and bromide-containing solutions. Equation (1) is a simplified equation for the underlying process.[3]

$$Au + 2Br^- + Br_2 \leftrightarrow AuBr_4^- + e^- \quad E_0 = +0{,}95V \qquad (1)$$

Bromide induces aggregation as well as dissolution of gold nanoparticles (see Intro-

duction). Even for purely sterically stabilized, monothiol functionalized gold particles, oxidation and complete dissolution were reported for bromide concentrations > 0.2 M when oxygen is present.[9] Note that in this case the particles were prepared by an approach with chloroauric acid as precursor, which likely limits their stability.[9, 23] All presented experiments were conducted under air atmosphere.

However, in the present case, already the only monovalent stabilized particles are highly stable in NaBr solutions. Even in a 2 M NaBr solution, the absorbance spectra are only slightly changing with time. Within 90 min the total intensity of the spectra slightly decreases, however, neither a significant broadening nor a shift of the absorbance maximum is found (see Figure 2 (a)). An increase of the reaction temperature from 25 to 45°C accelerates this decrease of the absorbance intensity (see Figure 2 (b)) but in contrast to the results reported in refs. [6, 7, 9] no broadening or shift of the absorbance maxima[6, 7] nor signs of significant dissolution[9] are found. This observation suggests that some aggregation and subsequent precipitation occurs. For a comparison, the decrease of the absorption maximum, normalized to its initial value, as a function of time is shown for different temperatures in Figure 2 (c). Since the observed spectral changes indicate that aggregation is the dominant process, the kinetics of this process was fitted by a mono-exponential function (cf. Equation (2)). This function typically describes slow colloidal aggregation in the reaction limited cluster aggregation (RLCA) regime, where the stability barrier is much higher than k_BT.[25, 26]

$$R(t) = R_\infty - A_1 e^{-k_1 t} \qquad (2)$$

Here, R(t) is the time dependent aggregation factor, R_∞ is R(t) for $t \rightarrow \infty$, A_1 is the amplitude, and k_1 is the rate constant of the aggregation process. The data can be well described by this fit (correlation coefficient $R \geq 0.98$). The results from fitting the aggregation data shown in Figure 2 (c) by using Equation (2) are summarized in Table S1 in the Supporting Information. For small gold particles of about 5 nm diameter, the plasmon oscillation is strongly damped and the absorption spectrum becomes weak and broad, hence, small changes in the particle size or polydispersity neither influence the shape nor the spectral position of the maximum of the plasmon resonance spectra.[27] Therefore, the time-dependent change of the monovalent stabilized particles in 2 M aqueous solutions of NaBr was also investigated by TEM. These samples which were taken during the UV-VIS measurements (see Figure 3). At 25°C, most particles remain unchanged, some are slightly grown and a few small particles are found, so that the total polydispersity slightly increases (see Figure 3 (a) and (b)). At 35°C (see Figure (3(c)) and 45°C (see Figure 3 (d)), this effect is more pronounced. However, the average diameter increases only about 1 nm after 90 min under these conditions, so that the effect on the plasmon resonance spectrum is rather negligible. All particles are still spherical, thus, some particles are shrinking while others are growing which is typical for an Ostwald ripening process.[9] As ICP-OES data indicate some gold ions were found in solution separated from the nanoparticles after 90 min of treatment with 2 M NaBr at 25°C. Thus, a small amount gold ions are released after the exposure to bromide, and hence, such a ripening process can take place.

Multivalent stabilized particles are even significantly more stable against aggregation. For divalent functionalized particles in 2 M NaBr solution for example neither a decrease nor a shift of the absorbance maximum or a time-dependent broadening

of the spectra was found. For comparison, these data are also added to Figure 2 (c).

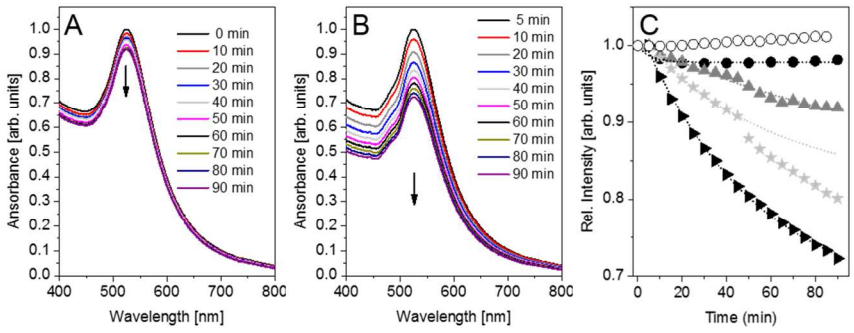

Figure 2. (a) Time-dependent changes of absorbance spectra of monothiol PEG-stabilized gold nanoparticles in a 2 M aqueous solution of NaBr (a) at 25°C and (b) at 45°C. (c) Time-dependent decrease of the intensity at the extinction maximum of the same particles in 2 M NaBr solution at 15°C (black circles), 25°C (dark grey triangles), 35°C (light grey stars), and 45°C (black triangles) as well as dithiol PEG-stabilized gold nanoparticles in 2 M NaBr solution at 35°C (open black circles). The data were fitted by a monoexponential function (see Equation (2)). Results of these fits are summarized in Table S1 in the Supporting Information.

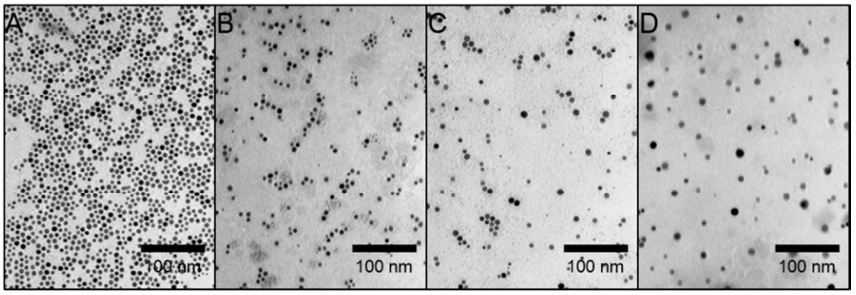

Figure 3. TEM images of monothiol PEG-stabilized gold nanoparticles from a 2 M aqueous solution of NaBr after (a) 5 min at 25°C, (b) 90 min at 25°C, (c) 90 min at 35°C, and (d) 90 min at 45°C.

An increase of the concentration accelerates the aggregation process of the monovalent stabilised particles (see Figure 4 (a)), but for NaBr concentrations of up to 4.5 M a significant broadening of the plasmon resonance band was not found. In 3 M solutions of NaBr the data can be still fitted by a monoexponential fit, whereas the data for the 4.5 M solution have to be fit by a biexponential function (Equation 3):

$$R(t) = A_1 e^{-k_1 t} - A_2 e^{-k_2 t} \qquad (3)$$

Here, R(t) is the time dependent aggregation factor, A_1 and A_2 are the amplitudes, and k_1 and k_2 are the rate constants of the two aggregation processes. ICP-OES measurements confirm that in NaBr solutions in contrast to NaCl the Au:S ratio of the nanoparticles increases. Thus, a significant amount of the ligands is replaced which agrees well with the observation that aggregation and Ostwald ripening processes are more enhanced in NaBr solutions.

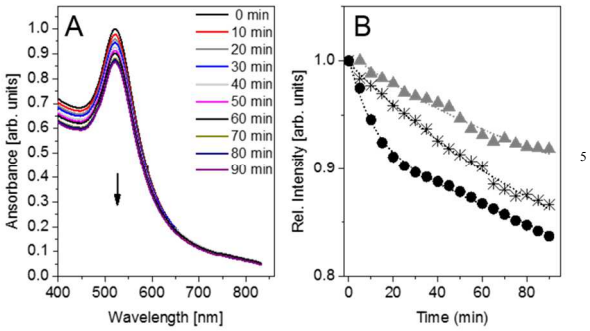

Figure 4. (a) Time-dependent changes of absorbance spectra of monothiol PEG-stabilized gold nanoparticles in a 3 M aqueous solution of NaBr and (b) time-dependent decrease of the intensity at the extinction maximum of the same particles in 2 M (dark grey triangles), 3 M (black stars), and 4.5 M (black solid spheres) aqueous solutions of NaBr. All spectra are measured at 25°C.

Studies in NaI

As discussed above iodide has the highest affinity to gold and, besides aggregation, can also induce Ostwald ripening and possibly fusion of gold nanoparticles. In the present studies all experiments were carried out in air. Hence, it must be taken into account that iodide is slowly oxidized in aqueous solutions by oxygen, carbon dioxide, and UV radiation to iodine (see Equation (4)).[28] The oxidation of iodide to iodine is also catalysed by gold surfaces.[29, 30]

$$4KI + 2CO_2 + O_2 \rightarrow 2K_2CO_3 + 2I_2 \qquad (4)$$

Iodine and iodide react to form triiodide (see Equation (5)), with the equilibrium constant $K = [I^-]\cdot[I_2]/[I_3^-] = 1.5\cdot10^{-3}$ mol/l.[31]

$$I^- + I_2 \leftrightarrow I_3^- \qquad (5)$$

Solutions containing iodide and triiodide can dissolve gold. The following reaction takes place (see Equation (6)):[31]

$$I^- + I_3^- + 2Au \leftrightarrow 2AuI_2^- \qquad (6)$$

Gold (I) compounds may be further oxidized to stable gold (III) iodide, depending on the given concentrations of the individual components.[3] Similar to Equation (1) for bromide, the chemical dissolution of gold in iodine-iodide-containing solutions can be described by the following overall reaction (Equation (7)):[3]

$$Au + 2I^- + I_2 \leftrightarrow AuI_4^- + e^- \qquad E_0 = +0{,}69V \qquad (7)$$

At concentrations ≤1 M NaI has only a small effect on the stability of mono- or multivalent stabilized gold nanoparticles (see Figure 7 (a)). However, for higher concentrations the presence of iodide induces a dramatic change of the spectral

properties of the monovalent stabilized nanoparticles, as it is shown in Figures 5 (a) – (c). In contrast to the results found for NaBr, even at low temperatures (15°C) the spectra are significantly shifted and broadened. This process becomes much faster if the temperature is raised from 15°C to 25°C where not only a broadening but also a significant change of the shape of the spectrum is found. This process is initially even more accelerated at 35°C but after 20 min only slight chances of the spectral shape occur and just the total intensity is slightly decreasing. At 45°C (spectra not shown), almost the same behaviour is observed.

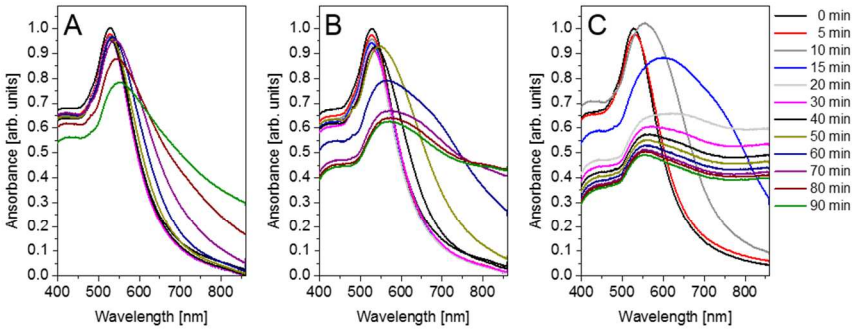

Figure 5. (a) Time-dependent changes of absorbance spectra of monothiol PEG-stabilized gold nanoparticles in a 2 M aqueous solution of NaI at (a) 15°C, (b) 25°C, and (c) 35°C.

For a comparison of the temporal changes of the absorbance spectra of the nanoparticles at different temperatures, a spectral broadening factor R was calculated which is defined as the ratio between the absorbance at 616 nm and the absorbance of the surface plasmon band (~524 nm) because changes in solution absorbance due to growth and aggregation processes were most noticeable at these two wavelengths in the measured spectra.[32, 33] In contrast, to the results for NaBr the process in NaI cannot be described by an exponential function. Thus, simple colloidal aggregation is no more the major process. For low temperatures (15°C), the time-dependent change of R appears to correspond to a sigmoidal growth process, but the data for higher temperatures show that this process is overlain by a second exponential decay process. Thus, an additional narrowing process occurs after some time (see Figure 6). The onset of this second process becomes more important for temperatures at or slightly above 25°C. Note that for different particle batches the onset of this process varies, even if the other characteristics (diameter and zetapotential of the particles, as well as width and maximum of the absorbance spectrum) are almost identical (see light grey solid stars and dark grey triangles in Figure 6 corresponding to two otherwise almost identical batches at 25°C in a 2 M solution of NaI). For identical batches this process is highly reproducible (see light grey circles and stars corresponding to two measurements of the same batch at 25°C in a 2 M solution of NaI).

A sigmoidal curve is typical for a kinetic process, where an initial induction period is followed by a regime of rapid growth, further growth, and final reaching of a saturation state. In case of the gold nanoparticles in the aqueous NaI solution, the induction step is the reaction of iodide of the initially highly stable nanoparticles, which results in a release or oxidation of the thiol PEG ligands as well as the release of gold ions or gold ion complexes (see Equations (4) – (7)). For fitting the sigmoidal process, we used initially a modified form of the Avrami-Erofe'ev equation

(Equation (8)).[34-36] This model applies rigorously to sigmoidal kinetics of specific types of solid-state phase transformation;[37, 38] but also have been used more recently for solution-based nucleation and growth processes of nanocrystals.[39, 40] There, the initial step is the nucleation. For the reaction of metal nanoparticles with halides sigmoidal kinetics have not been observed, likely because usually electrostatically stabilized particles were studied, where colloidal aggregation is the dominant process and further processes like fusion occur when the system is already heavily aggregated.[18]

$$R(t) = R_0 + B\left[1 - exp\left(-k_g t\right)^n\right] \quad (8)$$

Here, R(t) is the time-dependent spectral broadening factor, R_0 is R(t) for t =0, and R_0+B = R(t) for t→∞, k_g is the rate constant and n is the so-called Avrami exponent. For solid-state phase transformation kinetics, the parameter n is related to the mechanism of nucleation and the dimensionality of growth.[34-37] However, in nanocrystal growth processes, there is no physical interpretation for the parameter n.[39] The rate constant k_g in this model originates from a convolution of nucleation steps and growth steps and for nucleation/growth processes it was found that k_g strongly correlates with the growth rates and is rather insensitive to nucleation.[39, 41, 42]

In our case, Equation (8) yields a relative good agreement between measured and fitted data (R = 0.998-0.999) for the data obtained at low temperatures (≤ 25°C) and concentrations (≤2 M, see below), where the additional decay process is not too strong (see Figure S3 in the Supporting Information). Because of the lack of a precise physical meaning to the parameters k_g and n in this fit model and the fact, that this model contains only a single rate parameter for several processes, i. e. one of several activation and a growth process, we used a more recent model for fitting sigmoidal functions. This is the Finke-Watzky Two-Step Kinetic model, which has been successfully applied to several sigmoidal kinetics especially growth processes of metallic nanoparticles[43]. This two-step kinetic scheme consists of a nucleation step with a rate constant k_1 followed by autocatalytic growth with the rate constant k_2, see Scheme 1.[43]

$$A \xrightarrow{k_1} B$$
$$A + B \xrightarrow{k_2'} 2B$$

Scheme 1. Finke-Watzky two-step kinetic model of nucleation (k_1) and autocatalytic growth (k_2')[43]

In case of the gold nanoparticles in an iodide solution this first step can be interpreted as the step were reactive gold species are formed. Thus, unprotected gold atoms are formed because an oxidation process with I^- results in both the release (and possible additional oxidation) of the thiol PEG ligands, leaving the remaining gold atoms at the surface unprotected, and the release of gold ions into the solution. These processes are summarized to one activation step. The second step is the growth of the gold particles (see Scheme 2) where the activated gold particles grow and possibly also fusion processes occur:

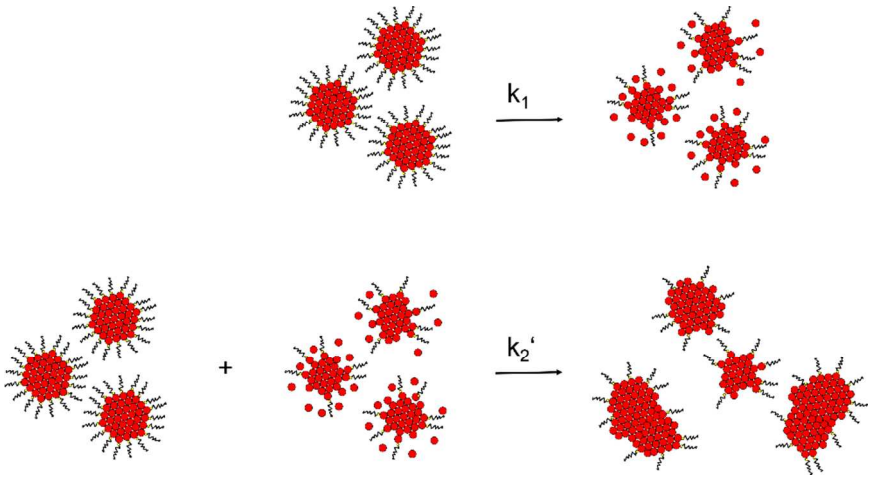

Scheme 2. Two-step model for the growth process of the gold nanoparticles in the presence of iodide in agreement with the Finke-Watzky two-step kinetic model.

This model allows a physically more reasonable interpretation of the data, since two rate constants, one for the activation and one for the growth, are obtained. Finney and Finke have shown that the Avrami model and the Finke-Watzky Two-Step kinetic model are in principle equivalent, however, the latter model yields kinetic parameters for both processes.[41] In the Finke-Watzky two-step kinetic model the integrated rate equation for the loss of A over time is given as Equation (9) (for the integration see ref. [43]):

$$[A] = \frac{\frac{k_1}{k_2'} + [A]_0}{1 + \frac{k_1}{k_2'[A]_0} exp[(k_1 + k_2'[A]_0)t]} \qquad (9)$$

Setting $\alpha = ([A]_0 - [A])/[A]_0$ and solving the equation to α, where α is the amount of starting material transformed into product yields Equation (10)

$$\alpha = 1 - \frac{k_1+k_2}{k_2+k_1 exp[(k_1+k_2)t]} \qquad (10)$$

Here, $k_2 = k_2'[A]_0$, this replacement removes the concentration dependences from the Finke-Watzky two-step kinetic model. This is needed since concentration is not a suitable concept in the solid-state.[41] In the present case, R(t), the time-dependent spectral broadening factor which is proportional to the fraction of particles grown larger and thus to α, hence, we set:

$$R(t) = R_\infty - A_1 \frac{k_1+k_2}{k_2+k_1 exp[(k_1+k_2)t]} \qquad (11)$$

Here, R(t) is the time-dependent spectral broadening factor, R_∞ is R(t) for t $\rightarrow\infty$ and R_∞ - A_1 is R(t) for t =0, k_1 is the rate constant for the first (activation) step. k_2 is the rate constant of the second (growth) process. Equation (11) yields a fit of similar quality as Equation 8 (see Supporting Information), but in contrast to Equation (8) it contains two time constants, one for the activation and one for the growth of the particles. However, none of the kinetic curves can be described purely by a sigmoid-

al growth process, especially at higher temperatures (see Figure 6 and 7), where some narrowing of the spectra takes place in a later state. This observation agrees well with the results from Morita et al., which shows that during fusion growth of gold nanoparticles a shrinkage of initially formed aggregates occurs due to the fusion processes which results in a decrease of the average particle size in the growth process. [22] For the present data, this decay process can be described by a simple exponential decay and in combination with the sigmoidal process described by Equation (11), Equation (12) results:

$$R(t) = R_\infty + A_1 \frac{k_1+k_2}{k_2+k_1 exp[(k_1+k_2)t]} + A_2 exp(-k_3 t) \qquad (12)$$

Here, R(t) is the time-dependent spectral broadening factor, R_∞ is R(t) for t $\rightarrow\infty$ and k_1 is the rate constant for the first (activation) step, k_2 is the rate constant of the second (growth) process (see Equation 11) and k_3 is the rate constant of the additional exponential decay process. A_1 and A_2 are the amplitudes of the sigmoidal and the exponential process, respectively.

With Equation (12) all kinetic data for NaI concentrations > 1 M can be well fitted (R >0.9889, see Table S2 and Figures 6 and 7). The rate constants for the first process (k_1) are about two orders of magnitude lower than those of the second process (k_2). Both rate constants increase with temperature. The rate constant of the additional decay process, k_3, is very small at low temperatures and increases strongly with increasing temperature. A combination of Equation (8) with an exponential decay process yields fits of equivalent quality (see Equation S1 and Figure S3 in the Supporting Information), but again with the limitation that the rate constant of the sigmoidal process has no real physical meaning.

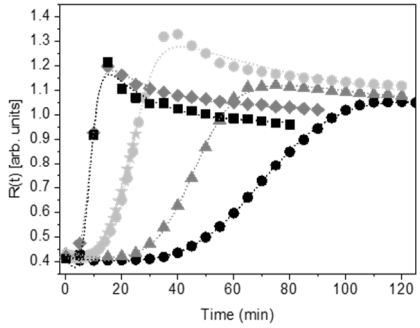

Figure 6. Time-dependent changes of the spectral broadening factor R (absorbance at 616 nm and 524 nm) of monothiol PEG-stabilized gold nanoparticles in a 2 M aqueous solution of NaI at 15°C (black circles), 25°C (dark grey triangles), 35°C (black solid squares), and 45° (dark grey diamonds). The light grey solid circles and stars are for another batch of monothiol PEG-stabilized particles also at 25°C (see also Figure S4 in the Supporting Information). The data are fitted by Equation (12). The results of the fits are summarized in Table S2 in the Supporting Information

For up to 1 M aqueous solutions of NaI at 25°C only a slight decrease of the intensity of the absorbance but no significant spectral changes are observed (see Figure 7 (a)), for higher concentrations a significant broadening of the spectra is found which is slowly starting at a concentration of 1.25 M (see Figure 7 (b)). The time-dependent change of the spectral broadening factor R(t) can be described well again

by the Equations (12) or (S1) (see Figure 7 (b) and Table S2 as well as Figure S3 (b) in the Supporting Information).

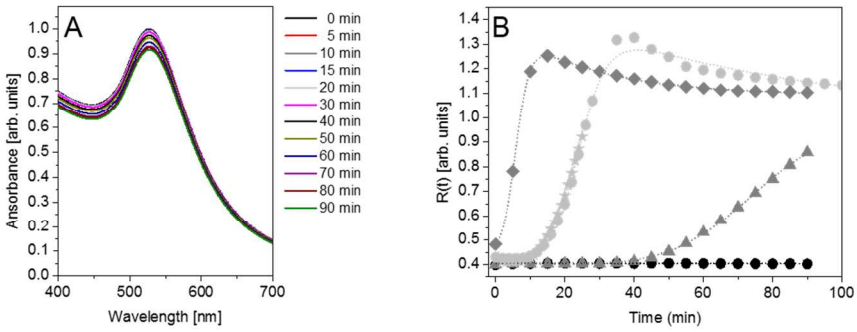

Figure 7. (a) Time-dependent changes of absorbance spectra of monothiol PEG-stabilized gold nanoparticles in a 1 M aqueous solution of NaI at 25°C and (b) time-dependent changes of the spectral broadening factor R(t) (R is the ratio between the absorbance at 616 nm and 524 nm) of monothiol PEG-stabilized gold nanoparticles at 25°C in 1 M (black circles), 1, 25 M (dark grey triangles), 2 M (light grey circles and light grey stars), and 3 M (dark grey diamonds) aqueous solutions of NaI. The data are fitted by Equation (12). The results of the fits are summarized in Table S2 in the Supporting Information.

ICP-OES measurements (see Table 1) confirm that more thiol ligands are replaced than in NaBr or NaCl solutions. After 24 h it was not possible to detect a proper Au:S ratio because a large amount of gold was released into the salt solution and the remaining amount of Au was below the detection limit.

TEM images of the corresponding samples show several effects of NaI on the gold nanoparticles: In the beginning, when the spectral broadening factor R(t) is only slightly increased, mostly spherical and slightly grown and shrinked particles as well as aggregates are found (see Figure 8 (a)). After longer reaction times, when R(t) has strongly increased, the average particle diameter also strongly increases to about 50-60 nm with a polydispersity of 30-50% (see Figures (8) (b) and statistical distributions of the particle diameters for the measurements at 35°C and 45°C in Figure S4 in the Supporting Information). After that the average diameter of the particles and the poly-dispersity slightly decreases but still remains high (> 30%) (see Figure 8 (c) and statistical distributions of the particle diameters in Figure S (4)). This slight reduction of the size and size distribution corresponds well to the exponential decay of the spectral broadening factor R(t) observed at higher temperatures (see Figure 6). In this advanced state, besides spherical particles, also some anisotropic (about 10%) particles like rods, triangular-prismatic, and hexagonal shapes are found, but most particles have still a more or less round shape (see Figure 8 (b)-(e)). Hence, strongly directed growth mechanisms as they are discussed for gold particles in the presence of iodide are not the major growth processes.[11-14] Notably, the iodide concentration is 4-5 orders of magnitude higher than in typical directed growth syntheses in the presence of iodide.[11-14] Please note, that the large, rather bright prismatic structures in Figure 8 (c) marked with an asterisk are NaI and not Au, such structures were found in all samples and were identified as iodide by EDX. For TEM imaging most NaI was washed off from the samples, but a complete removal was not possible. Additionally, to the anisotropic structures, some irregular shaped particles are ob-

served (marked with an arrow in the Figures 8 (c) – (e)). HRTEM images (Figures 8 ((f) – (j)) reveal that these irregular shaped particles and other particles still appearing more spherical consist of several parts with different crystalline orientations. This can be clearly recognized by alternating dark and bright fringes in the HRTEM images which are so-called Moiré fringes (interference fringes) which appear when two crystals with different lattice plane distances or orientations overlap.[44] The fact that such structures are found indicates that the particles are not just growing by a simple molecular growth process, but that also processes take place where two or more gold particles fuse together. Such a process has been already observed for electrostatically stabilized gold nanoparticles at much lower (2-3 orders of magnitude lower) NaI concentrations.[6, 8] Based on these observations, the following growth process can be postulated: In a slow induction period iodide reacts with the particles resulting in both the release of the PEG thiol ligands and a partial oxidation of the gold atoms, so that gold ions or gold –iodide complexes serving as monomeric precursors for further growth processes are formed in solution. With an increasing number of gold ions in solution, the particles start to grow and as the stabilizing ligands are partly released, aggregation processes occur. Free gold ions attach on these aggregates leading to the formation of larger irregularly shaped fused structures. Subsequently, the formation of the fused structures from the aggreagtes results in a slight narrowing of the size distribution and the width of the absorbance spectra.

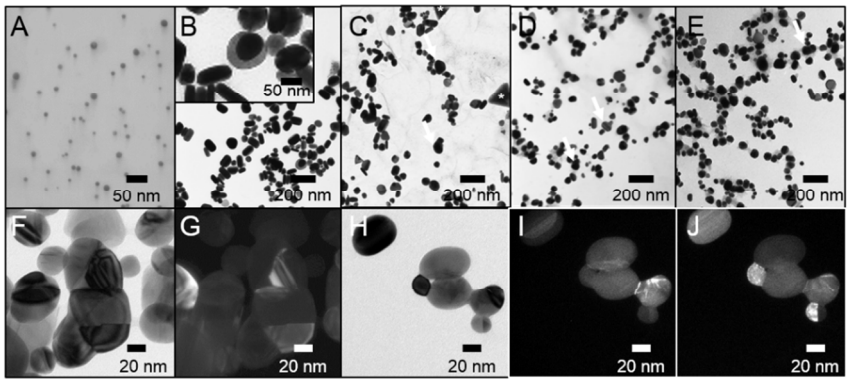

Figure 8. Top row: TEM images of monothiol PEG-stabilized gold nanoparticles in a 2 M aqueous solution of NaI after (a) 5 min at 35°C, (b) 45 min at 35°C, (c) 90 min at 35°C and (d) 5 min at 45°C, and (e) 45 min at 45°C. Bottom row: (f) and (h) bright field HRTEM images of fused gold particles and (g) as well as (I, j) corresponding dark field images of monothiol PEG-stabilized gold nanoparticles in a 2 M aqueous solution of NaI after 90 min at 45°C.

In case of the divalent stabilized particles, different results are obtained. Here, the presence of NaI causes only some broadening and a slight shift of the absorbance spectra (see Figure 9 (a)). TEM images indicate that neither a significant growth of the particles nor fusion processes occur (see Figure 9 (b)) Thus the divalent ligands provide such a strong stabilization that a considerable ligand exchange is not possible in agreement with the results for NaCl and NaBr.

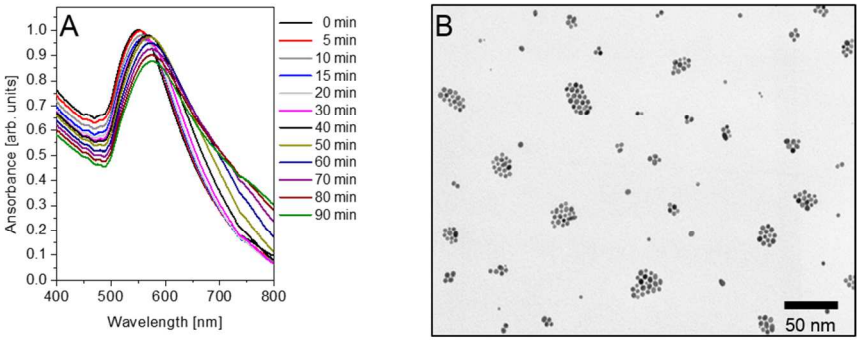

Figure 9. (a) Time-dependent changes of absorbance spectra of dithiol PEG-stabilized gold nanoparticles in a 3 M aqueous solution of NaI at 25°C and (b) TEM of the same particles after 90 min in the same solution at 25°C.

Experimental

All reactions for the preparation of the particles were conducted in flame- or oven-dried glassware under nitrogen atmosphere and were stirred magnetically. All microwave assisted particle-synthesis were carried out on the device CEM Discover. Nanoparticles were analysed by UV/vis absorption measurements performed with a Lambda 950 from PerkinElmer (The data analysis of the spectra was performed with OriginPro 8.6) and by TEM measurements on a Zeiss-EM-10-CR-TEM from Carl Zeiss with an acceleration voltage of 80 kV. At least 200 particles per sample were analysed to derive the size distributions of the samples. HRTEM images were obtained with a FEI Tecnai G² 20 S-TWIN at an acceleration voltage of 200 kV.

Inductively coupled plasma optical emission spectrometry (ICP-OES) measurements were carried out with an iCAP 6200 Duo from Thermo Fisher Scientific. After the reaction with the sodium halide solutions, the supernatant was separated from the remaining particles by centrifugation. The remaining sediment was dissolved in aqua regia. The sulphur in the supernatant as well as the gold content of the sediment were determined. The analyte wavelength were 242.7 und 267.5 nm for gold and 180.7 nm for sulphur.

Nanoparticle and Ligand Synthesis

The mono-and divalent ligands were prepared according to earlier procedures with slight modifications as described in ref. [23] The trivalent ligand was synthesized as de-scribed in ref. [23] The synthesis of $[NMe_4][Au(CF_3)_2]$ was carried out according to ref. [24]. "Naked" gold nanoparticles were prepared from $[NMe_4][Au(CF_3)_2]$ in a microwave apparatus.[24] The coordination of free particle surfaces was achieved by addition of aqueous solution of the mono-, di- , or trivalent thiol PEG ligands.[23].

Stability Studies

ThiolPEG functionalized Au NP were added to NaCl, NaBr, or NaI solutions, so that the final salt concentrations were 1-5 M and mixed thoroughly. All samples were adjusted to an optical density of 0.3 at the extinction maximum. Absorbance spectra were recorded in regular intervals depending on the reaction rate. The stability experiments were carried out at 15, 25, 35, and 45°C. All experiments with halides

were carried out in air.

Conclusions

The stability of 5-6 nm large gold nanoparticles in up to 5 M aqueous solutions of NaCl, NaBr, and NaI was systematically investigated. The particles were obtained by the in situ functionalization of gold nanoparticles from a Cl^--free synthesis with mono- and multivalent thiol polyethylene glycol (PEG) ligands. The purely sterically stabilized particles are stable against aggregation or any oxidative growth or dissolution process in up to 1 M NaCl and NaBr solutions regardless of the valence of the ligands. At higher concentrations (≥ 2 M) the monovalent stabilized particles show minor aggregation which can be described by slow colloidal aggregation in the regime of reaction limited cluster aggregation. In aqueous solutions of NaBr additionally an almost negligible Ostwald ripening process occurs which becomes slightly more important when the temperature is raised to 35°C or 45°C. However, even at T = 45°C or concentrations of up to 4.5 M the shape and the spectral position of the maximum of the plasmon resonance band of these particles do not change with time. In NaCl solutions an Ostwald ripening process is not observed. The divalent stabilized particles remain colloidally stable in both halide solutions even if the temperature is raised or the concentration is increased above 2 M. In aqueous NaI solutions the monovalent stabilized particles also remain stable for concentrations of up to 1 M, whereas electrostatically stabilized particles as well as sterically stabilized, thiol-protected gold particles from a synthesis with chloroauric acid as precursor show pronounced aggregation, dissolution, and fusion processes already at 2-3 orders of magnitude lower halide concentrations.[6, 9] At concentrations above 1.25 M the monovalent stabilized particles undergo an oxidative reactions with iodide which results in a time-dependent significant shift and broadening of the plasmon resonance spectrum. After long time periods this process slows down while the width of the spectra slightly narrows. The kinetics of this process can be described by sigmoidal process corresponding to a Finke-Watzky Two-Step kinetic model[41, 43] with an additional exponential decay term for the narrowing process. In the slow induction period, the first step, iodide reacts with the particles resulting in both the release of the PEG thiol ligands and a partial oxidation of the gold atoms on the particle surface resulting in a release of monomeric gold species into the solution. With an increasing number of gold ions in solutions the particles start to grow in the second step and as the stabilizing ligands are partly released, also aggregation takes place. Free gold ions attach onto the resulting aggregates which leads to the formation of larger, irregularly shaped fused structures. The formation of the fused structurs from the aggregates then results in a slight narrowing of the size distribution and consequently a reduction of the witdth of the absorbance spectra. The formation of an increasing number of fused structures could be confirmed by HRTEM. In case of the divalent stabilized particles different results are obtained. Here, the presence of up to 3 M NaI in aqueous solutions causes only some minor broadening and a slight shift of the absorbance spectra. This observation confirms the excellent stability of the multivalent stabilized particles from this chloride-free particle synthesis.

Acknowledgements

The authors acknowledge financial support for this research by SFB765-A4 and the Freie Universität Berlin. A. M. acknowledges for a scholarship from ERASMUS MUNDUS.

References

[a] *Address, Address, Town, Country. Fax: XX XXXX XXXX; Tel: XX XXXX XXXX; E-mail: xxxx@aaa.bbb.ccc*
[b] *Address, Address, Town, Country. Fax: XX XXXX XXXX; Tel: XX XXXX XXXX; E-mail: xxxx@aaa.bbb.ccc*

† Electronic Supplementary Information (ESI) available: Structures of the mono-, di-, and trivalent thiol PEG ligands, TEM image of the untreated particles, fit parameters of the fits shown in the Figures 2,4,6, and 7, further fits of the time-dependent changes of the spectral broadening factor R of PEG-stabilized gold nanoparticles in a 2 M aqueous solution of NaI at 15°C and a 3 M aqueous solution of NaI at 15°C. and an additional fit fuction for describing these data. Statistical distribution of the particle diameter of monothiol PEG-stabilized gold nanoparticles in a 2 M aqueous solution of NaI at (a) 35°C and (b) 45°C. See DOI: 10.1039/b000000x/

1. S. K. Ghosh and T. Pal, *Chem. Rev.*, 2007, **107**, 4797-4862.
2. R. G. Pearson, *J. Am. Chem. Soc.*, 1963, **85**, 3533-&.
3. J. H. Marsden, I.,, *The Chemistry of Gold Extraction*, Society for Mining, Metallurgy, and Exploration, Littleton, Colorado, 2006.
4. O. M. Magnussen, B. M. Ocko, R. R. Adzic and J. X. Wang, *Phys. Rev. B*, 1995, **51**, 5510-5513.
5. N. Almora-Barrios, G. Novell-Leruth, P. Whiting, L. M. Liz-Marzan and N. Lopez, *Nano Lett.*, 2014, **14**, 871-875.
6. Y. Liu, L. L. Liu and R. Guo, *Langmuir*, 2010, **26**, 13479-13485.
7. S. Singh, R. Pasricha, U. M. Bhatta, P. V. Satyam, M. Sastry and B. L. V. Prasad, *J. Mater. Chem.*, 2007, **17**, 1614-1619.
8. W. L. Cheng, S. J. Dong and E. K. Wang, *Ang. Chem. Int. Ed.*, 2003, **42**, 449-+.
9. M. Dasog and R. W. J. Scott, *Langmuir*, 2007, **23**, 3381-3387.
10. L. Pei, K. Mori and M. Adachi, *Colloid Surf. A-Physicochem. Eng. Asp.*, 2006, **281**, 44-50.
11. L. H. Pei, K. Mori and M. Adachi, *Langmuir*, 2004, **20**, 7837-7843.
12. D. K. Smith, N. R. Miller and B. A. Korgel, *Langmuir*, 2009, **25**, 9518-9524.
13. J. E. Millstone, W. Wei, M. R. Jones, H. Yoo and C. A. Mirkin, *Nano Lett.*, 2008, **8**, 2526-2529.
14. T. H. Ha, H.-J. Koo and B. H. Chung, *J. Phys. Chem. C*, 2007, **111**, 1123-1130.
15. B. V. Enüstün and J. Turkevich, *J. Am. Chem. Soc.*, 1963, **85**, 3317-3328.
16. S. S. Shankar, S. Bhargava and M. Sastry, *J. Nanosci. Nanotechno.*, 2005, **5**, 1721-1727.
17. K. A. Huynh and K. L. Chen, *Environ. Sci. Technol.*, 2011, **45**, 5564-5571.
18. A. M. El Badawy, K. G. Scheckel, M. Suidan and T. Tolaymat, *Sci. Total Environ.*, 2012, **429**, 325-331.
19. N. Kallay and S. Zalac, *J. Colloid Interf. Sci.*, 2002, **253**, 70-76.
20. T. Kim, C.-H. Lee, S.-W. Joo and K. Lee, *J. Colloid Interf. Sci.*, 2008, **318**, 238-243.
21. R. Pamies, J. G. Hernandez Cifre, V. Fernandez Espin, M. Collado-Gonzalez, F. G. Diaz Banos and J. Garcia de la Torre, *J. Nanopart. Res.*, 2014, **16**.
22. T. Morita, K. Kurihara, O. Yoshida, H. Imamura, Y. Hatakeyama, K. Nishikawa and N. Uehara, *J. Phys. Chem. C*, 2013, **117**, 13602-13608.
23. D. Zopes, B. Stein, S. Mathur and C. Graf, *Langmuir*, 2013, **29**, 11217-11226.
24. D. Zopes, S. Kremer, H. Seherer, L. Belkoura, I. Pantenburg, W. Tyrra and S. Mathur, *Eur. J. Inorg. Chem.*, 2011, 273-280.
25. M. Y. Lin, H. M. Lindsay, D. A. Weitz, R. C. Ball, R. Klein and P. Meakin, *Phys. Rev. A*, 1990, **41**, 2005-2020.
26. Z. K. Zhou and B. Chu, *Physica A*, 1991, **177**, 93-100.
27. S. Link and M. A. El-Sayed, *Int. Rev. Phys. Chem.*, 2000, **19**, 409-453.
28. P. A. Lyday, in *Ullmann's Encyclopedia of Industrial Chemistry*, Wiley-VCH Verlag GmbH & Co. KGaA, Berlin, 2000.

29. J. F. Rodriguez, T. Mebrahtu and M. P. Soriaga, *J. Electroanal. Chem.*, 1987, **233**, 283-289.
30. M. A. Tadayyoni, P. Gao and M. J. Weaver, *J. Electroanal. Chem.*, 1986, **198**, 125-136.
31. P. H. Qi and J. B. Hiskey, *Hydrometallurgy*, 1991, **27**, 47-62.
32. B. C. Mei, E. Oh, K. Susumu, D. Farrell, T. J. Mountziaris and H. Mattoussi, *Langmuir*, 2009, **25**, 10604-10611.
33. V. Amendola and M. Meneghetti, *J. Mater. Chem.*, 2007, **17**, 4705-4710.
34. M. Avrami, *J. Chem. Phys.*, 1939, **7**, 1103.
35. M. Avrami, *J. Chem. Phys.*, 1940, **8**, 212.
36. M. Avrami, *J. Chem. Phys.*, 1941, **9**, 177.
37. A. A. Burbelko, E. Fras and W. Kapturkiewicz, *Materials Science and Engineering a-Structural Materials Properties Microstructure and Processing*, 2005, **413**, 429-434.
38. L. E. Levine, K. L. Narayan and K. F. Kelton, *J. Mater. Res.*, 1997, **12**, 124-132.
39. F. D. Wang, V. N. Richards, S. P. Shields and W. E. Buhro, *Chem. Mat.*, 2014, **26**, 5-21.
40. M. Drofenik, M. Kristl, A. Znidarsic, D. Hanzel and D. Lisjak, *J. Am. Cer. Soc.*, 2007, **90**, 2057-2061.
41. E. E. Finney and R. G. Finke, *Chem. Mater.*, 2009, **21**, 4692-4705.
42. S. P. Shields, V. N. Richards and W. E. Buhro, *Chem. Mat.*, 2010, **22**, 3212-3225.
43. M. A. Watzky and R. G. Finke, *J. Am. Chem. Soc.*, 1997, **119**, 10382-10400.
44. K.-W. Benz and W. Neumann, *Introduction to Crystal Growth and Characterization*, Wiley-VCH, Weinheim, 2014.

Table of contents entry:

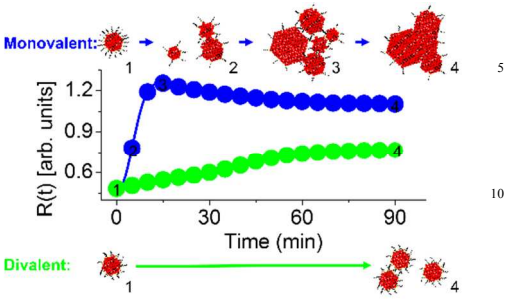

Gold nanoparticles from a chloride-free synthesis exhibit excellent stability in concentrated halide solutions. In NaI solutions, particles with monovalent ligands undergo slow activation, fast growth and aggregation, and finally fusion, whereas divalent stabilized particles only slightly aggregate.

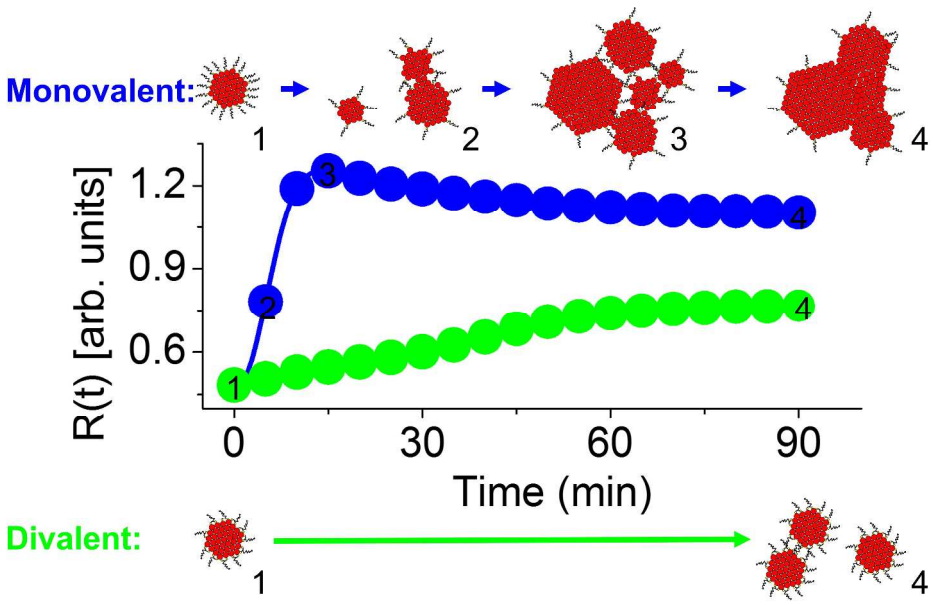

1047x642mm (150 x 150 DPI)